Contribution from the Departments of Chemistry, Calvin College, Grand Rapids, Michigan 49506, and University of Calgary, Calgary, Alberta, Canada T2N 1N4

Structure and Fragmentation of Ag_2H^+ and $Ag_2CH_3^+$

Roger L. DeKock,*† Roger D. van Zee, and Tom Ziegler*‡

Received July 22, 1986

Hartree-Fock-Slater calculations were completed on the title ions. Both of these three-center two-electron bond systems are calculated to be triangular with the proton or the methyl group bridging a lengthened (~0.1 Å) Ag_2 bond. The proton affinity of Ag_2 is calculated to be 193.5 kcal/mol and the methyl cation affinity is 128.7 kcal/mol. A bond energy decomposition analysis reveals that the lower methyl cation affinity results from the larger steric interaction of the methyl cation with the Ag_2 fragment and from the energy required to make the methyl cation pyramidal in order to prepare it for bonding to the Ag_2 fragment. The fragmentation energies of the ions are calculated, and the results are discussed with respect to the collision-induced-dissociation work of Busch et al.

Introduction

The impetus for this study was provided by the tandem mass spectrometry work of Busch et al.[1] and by our interest in the three-center two-electron (3c-2e) chemical bond.[2] The collision-induced dissociation (CID) revealed that most ions of formula Ag_2X^+ dissociate with a significant percentage to the silver dimer ion Ag_2^+ but that Ag_2H^+ and Ag_2OH^+ do not do so. This was interpreted as an indication that the former category, including $Ag_2CH_3^+$, contain metal-metal bonds whereas Ag_2H^+ and Ag_2OH^+ do not. Although not stated explicitly in ref 1, the implication is that the *fragmenting ions* have a different structure for Ag_2H^+ than for $Ag_2CH_3^+$. A point of discussion that we shall take up below is whether or not this has any relationship to the *ground-state* structure.

A simple view of molecules containing unsupported 3c-2e bonds leads one to predict that all of them should be bent or triangular, and consequently all should have a metal-metal bond to a greater or lesser extent.[2,3] (This conclusion would not apply to Ag_2OH^+, since this ion has the same topology as H_3O^+ and does not contain a 3c-2e bond.) Recently, an X-ray structure of a silver-carborane salt has shown this compound to contain a bent 3c-2e AgHB bond.[4] Molecular pseudopotential calculations on Ag_2H^+ also predict this species to be triangular.[5] A linear structure is expected only in the event that steric effects are more important than electronic effects. Such apparently is the case in the predicted linear structure of the corresponding group 1 systems M_2H^+.[6] Evidently, the large partial positive charge on the metal atoms forces these cations to be linear,[7] in spite of a lowering of the electronic portion of the energy in the triangular framework.

The *topology* of these systems is of as much interest as the *structure*. In general, the most stable topology is the one that places the most electronic charge on the most electronegative atoms.[8] The 3c-2e bond results in a buildup of charge at the central atom, and hence the most stable topology should be that with the H atom in the central position for the M_2H^+ ions.

Because of our interest in the simple structure/topology considerations discussed above, we set out to calculate the structure of the ground electronic state of the title ions as well as the group 1 ion Li_2H^+. The tandem mass spectrometry work[1] led us to calculate the fragmentation energies of the title ions as well. We chose the Hartree-Fock-Slater (HFS) method[9] since it is known to provide results in good agreement with experiment for diatomic molecules of the second- and third-row transition-metal elements. We examined both topologies $AgXAg^+$ and $AgAgX^+$. Our HFS calculations coupled with the Ziegler transition state energy analysis method[10] allows us to calculate the proton affinity and the methyl cation affinity of the diatomic Ag_2 molecule. This analysis provides a useful breakdown into steric and electronic effects of the total interaction energy between fragments in a molecule or ion. The HFS method recently has been used to examine the angular geometry of main-group-element molecules.[11]

In the course of our study we repeated HFS calculations[12] on AgH and Ag_2. These molecules as well as the Au congeners have come under concerted study lately,[13] for reasons having to do with testing new computational schemes for heavy-metal systems and for developing methods that might be used in cluster studies. There also is one report on the bonding of methyl groups in dinuclear transition-metal compounds that compares terminal, symmetrical bridging, and asymmetrical bridging geometries.[14]

Calculations

We have carried out calculations on Li_2H^+, Ag_2, AgH, $AgCH_3$, Ag_2H^+, and $Ag_2CH_3^+$ using the HFS method.[9] Geometry optimizations were carried out in a series of linear searches without the use of energy gradient techniques; bond distances reported with two significant figures should only be considered correct within the approximations of the HFS method to ±0.05 Å. We did not optimize the CH_3 geometry, but chose standard bond lengths (1.09 Å) and angles (109°). This certainly will be a reasonable geometry for the topology $AgAgCH_3^+$ and on the basis of the structures of bridging methyl systems should be suitable there also.[14,15] The point group symmetries in which these molecules were studied are as follows: Ag_2, $D_{\infty h}$; AgH, $C_{\infty v}$; $AgCH_3$, C_{3v}; Ag_2H^+, C_{2v}; $Ag_2CH_3^+$, C_s.

The basis set was double ζ on the C and H atoms; the H atom also had a single-ζ 2p orbital. A triple-ζ basis set was employed on the Ag atom with a triple-ζ 5p orbital as well. The cores Ag(1s-3d) and C(1s) were kept frozen; the valence orbitals were orthogonalized onto the core.

† Calvin College.
‡ University of Calgary.

(1) Busch, K. L.; Cooks, R. G.; Walton, R. A.; Wood, K. V. *Inorg. Chem.* **1984**, *23*, 4093.
(2) DeKock, R. L.; Dutler, R.; Rauk, R.; van Zee, R. D. *Inorg. Chem.* **1986**, *25*, 3329. DeKock, R. L.; Bosma, W. B., submitted for publication in *J. Chem. Educ.*
(3) Bau, R.; Teller, R. G.; Kirtley, S. W.; Koetzle, T. F. *Acc. Chem. Res.* **1979**, *12*, 176. Shore, S. G.; Lawrence, S. H.; Watkins, M. I.; Bau, R. *J. Am. Chem. Soc.* **1982**, *104*, 7669. Raghavachari, K.; Schleyer, P. v. R.; Spitznagel, G. W. *J. Am. Chem. Soc.* **1983**, *105*, 5917. Sapse, A.-M.; Osorio, L. *Inorg. Chem.* **1984**, *23*, 627. Hart, D. W.; Bau, R.; Koetzle, T. F. *Organometallics* **1985**, *4*, 1590.
(4) Shelly, K.; Finster, D. C.; Lee, Y. L.; Scheidt, W. R.; Reed, C. A. *J. Am. Chem. Soc.* **1985**, *107*, 5955.
(5) Gaspar, R.; Tamassy-Lentei, I. *Acta Phys. Acad. Sci. Hung.* **1981**, *50*, 343.
(6) Raffenetti, R. C.; Ruedenberg, K. *J. Chem. Phys.* **1973**, *59*, 5978. Cardelino, B. H.; Eberhardt, W. H.; Borkman, R. F. *J. Chem. Phys.* **1986**, *84*, 3230.
(7) Jemmis, E. D.; Chandrasekhar, J.; Schleyer, P. v. R. *J. Am. Chem. Soc.* **1979**, *101*, 527.
(8) DeKock, R. L.; Gray, H. B. *Chemical Structure and Bonding*; Benjamin/Cummings: Menlo Park, CA, 1980; p 116.
(9) Baerends, E. J.; Ros, P. *Chem. Phys.* **1973**, *2*, 52. Baerends, E. J.; Ros, P. *Int. J. Quantum Chem. Symp.* **1978**, *12*, 169. Heijser, W.; Baerends, E. J.; Ros, P. *Faraday Discuss. Chem. Soc.* **1980**, *No. 14*, 211.
(10) Ziegler, T.; Rauk, A. *Theor. Chim. Acta* **1977**, *46*, 1. Ziegler, T.; Rauk, A. *Inorg. Chem.* **1979**, *18*, 1558, 1755.
(11) Trsic, M.; Laidlaw, W. G. *THEOCHEM* **1985**, *123*, 259. Laidlaw, W. G.; Trisic, M. *Can. J. Chem.* **1985**, *63*, 2044.
(12) Ziegler, T.; Snijders, J. G.; Baerends, E. J. *J. Chem. Phys.* **1981**, *74*, 1271.
(13) Rabii, S.; Yang, C. Y. *Chem. Phys. Lett.* **1984**, *105*, 480. Flad, J.; Igel-Mann, G.; Preuss, H.; Stoll, H. *Chem. Phys.* **1984**, *90*, 257. Cingi, M. B.; Clemente, D. A.; Foglia, C. *Mol. Phys.* **1984**, *53*, 301. Hay, P. J.; Martin, R. L. *J. Chem. Phys.* **1985**, *83*, 5174. Andzelm, J. *J. Chem. Phys.* **1985**, *83*, 4753. Ross, R. B.; Ermler, W. C. *J. Phys. Chem.* **1985**, *89*, 5202.
(14) Bursten, B. E.; Cayton, R. H. *Organometallics* **1986**, *5*, 1051.
(15) Holton, J.; Lappert, M. F.; Ballard, D. G. H.; Pearce, R.; Atwood, J. L.; Hunter, W. E. *J. Chem. Soc., Dalton Trans.* **1979**, 54.

0020-1669/87/1326-0563$01.50/0

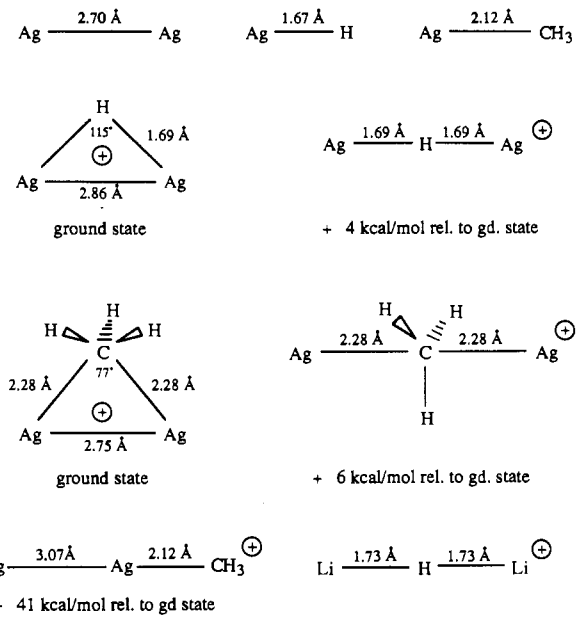

Figure 1. Structures and relative energies of the molecules and ions.

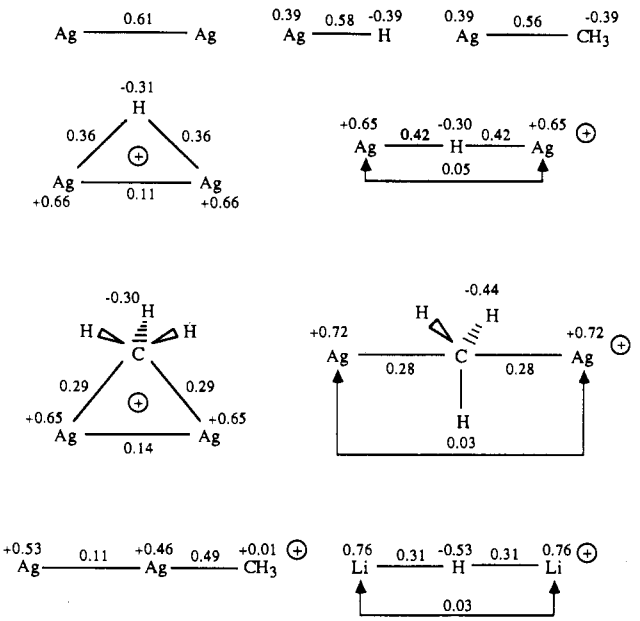

Figure 2. Mulliken atomic charges and overlap populations. The overlap populations involving the methyl group are with the carbon atom only.

All basis functions were uncontracted and were of the STO type. A standard value of $\alpha = 0.7$ was used for the exchange scale factor.

Ionization potentials and fragmentation energies were calculated for a number of molecules and ions in this study. All such energies were obtained by using the Ziegler transition state energy analysis method,[10] and the calculations were run unrestricted whenever this was necessitated by the electron count at hand. In no case did we employ the half-electron method of Slater to calculate the relevant ionization energies.

A few relativistic calculations were performed for Ag_2H^+. Such effects are known to be small for second-row transition elements compared to third row.[16] Because of this and the fact that we are doing a comparative study on Ag_2H^+ and $Ag_2CH_3^+$, we decided to ignore relativistic effects. On the basis of the limited relativistic work that we did as a part of this work and the results in the literature on Ag_2 and AgH, it appears that such effects shorten bond lengths by about 0.1 Å and increase bond dissociation energies by about 5–10 kcal/mol.

Results and Discussion

Structures and Relative Energies. In Figure 1 we present the calculated structures for all of the silver-containing molecules and ions that were studied as well as Li_2H^+. We also show the relative energies for the different structures and topologies of the ions. Our results for Ag_2 and AgH are in good agreement with a number of other calculations that are available in the literature.[12,13]

We calculate that Li_2H^+ is linear, in agreement with previous theoretical work on this ion.[6,7] The energy required to bend the triatomic ion to an angle of 140° is only about 2 kcal/mol.

The structure of the Ag_2H^+ ion is calculated to be triangular, in contrast to that of Li_2H^+. However, here again the bending deformation energy is small. The energy difference is only 4 kcal/mol between the most stable structure with a bond angle of 115° and the linear structure. In the triangular structure the Ag–Ag bond has lengthened by 0.16 Å compared to the Ag_2 molecule. We find that the calculated Ag–H bond length is the same whether the ion is linear or triangular. The fact that Ag_2H^+ is triangular whereas Li_2H^+ is linear is not too surprising when one considers that the experimental Li_2 bond strength is only 24 kcal/mol compared to 38 kcal/mol for Ag_2.[17] We also completed calculations on the $AgAgH^+$ topology and find it to be unstable with respect to the fragments AgH and Ag^+. Qualitatively, this can be interpreted as evidence that the HOMO (donor orbital) of AgH is strongly polarized toward the H end and hence there is little donor ability through the Ag end toward a formal Ag^+ acceptor.

Calculations on the $Ag_2CH_3^+$ cation indicate a topology and structure in close agreement with those of Ag_2H^+. It is interesting to note the structural similarity between the $Ag_2CH_3^+$ ion and CH_5^+.[18] The Ag–Ag bond length is about 0.1 Å shorter than that in Ag_2H^+; there is a 6 kcal/mol energy difference between the linear and triangular AgCAg frameworks. The Ag–C bond length optimizes to the same value in both structures, about 0.1 Å longer than in the $AgCH_3$ molecule. (In the linear structure we adopted a planar CH_3 group but did not optimize the C–H bond lengths.) The heavy-atom framework of $Li_2CH_3^+$ is linear Li–C–Li,[7] in contrast to the corresponding $Ag_2CH_3^+$ ion. The $AgAgCH_3^+$ topology is 41 kcal/mol less stable than the triangular triatomic, and the Ag–Ag bond has lengthened considerably.

In summary, there is close correspondence between the $Ag_2CH_3^+$ and Ag_2H^+ ions in structure and relative energies of alternative topologies. The main difference between the two is that there must be a large barrier to rearrangement for the $Ag_2CH_3^+$ ion in going from the linear AgCAg structure to the triangular, whereas the Ag_2H^+ ion has no barrier. We did not carry out calculations to explore this barrier height, since this would have necessitated optimization of CH_3 bond lengths and angles. This barrier height will result in a larger bending deformation energy for $Ag_2CH_3^+$ than for Ag_2H^+. As we shall see below, the energy required to fragment the $Ag_2CH_3^+$ ion into Ag^+ and $AgCH_3$ is calculated to be 63 kcal/mol. Hence, we estimate the barrier height to go from the triangular to the linear AgCAg structure to be on the order of 50 kcal/mol. (We do not anticipate that the Ag^+ ion will be able to garner more than about 13 kcal/mol bond energy as it migrates around the back side of the methyl group.)

Electronic Structure and Bonding of Ag_2H^+ and $Ag_2CH_3^+$. We next turn our attention to a brief analysis of the electronic structure and bonding of the silver-containing molecules and ions. In Figure 2 we exhibit the computed Mulliken atomic charges and overlap populations. It is clear that the bridging H atom of Ag_2H^+ has a large amount of electronic charge. For comparison purposes we have included also the data for Li_2H^+, and we see that the charge polarization is even larger than in the Ag_2H^+ ion. This is expected on the basis of the smaller electronegativity of Li compared to that of Ag. The individual Ag–H overlap populations in Ag_2H^+ are only a little more than half those in the diatomic AgH, no doubt related to the fact that we have gone from a 3c–2e bond to a 2c–2e bond. The same remark applies to the Ag–C overlap population in $Ag_2CH_3^+$ compared to that in $AgCH_3$.

(16) Pitzer, K. S. *Acc. Chem. Res.* **1979**, *12*, 271. Christiansen, P. A.; Ermler, W. C.; Pitzer, K. S. *Annu. Rev. Phys. Chem.* **1985**, *36*, 407.
(17) Huber, K. P.; Herzberg, G. *Molecular Spectra and Molecular Structure*; Van Nostrand Reinhold: New York, 1979; Vol. IV.
(18) Fois, E.; Gamba, A.; Simonetta, M. *Can. J. Chem.* **1985**, *63*, 1468.

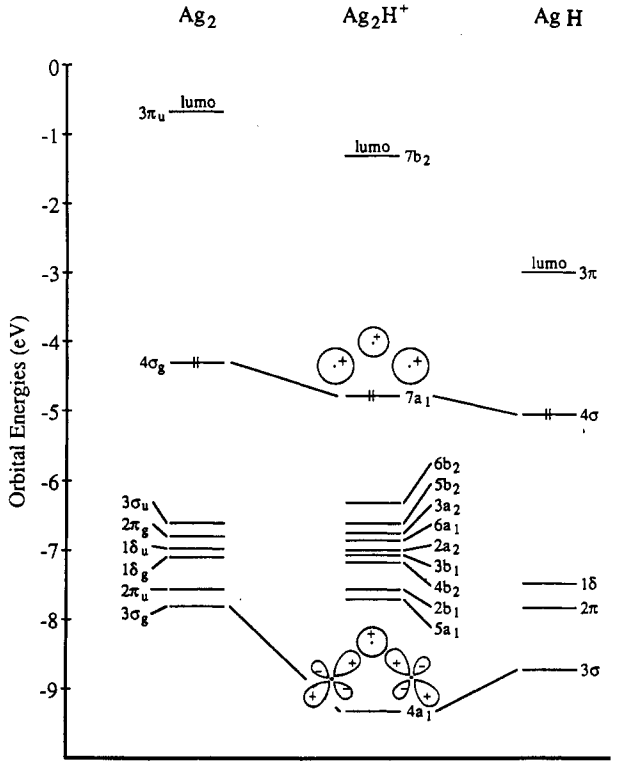

Figure 3. Molecular orbital correlation diagram for Ag_2, Ag_2H^+, and AgH.

The Ag–Ag overlap population is decidedly less in both Ag_2H^+ and $Ag_2CH_3^+$ than in the diatomic Ag_2. Calculations on Ag_2 at the same bond length that is present in Ag_2H^+ reveals that the overlap population has dropped only slightly from 0.614 in free Ag_2 to 0.586 in "lengthened" Ag_2. Hence, the major part of the decrease in Ag–Ag overlap population is due to withdrawal of electronic charge by the bridging group. From such overlap population numbers it is difficult to state the extent of Ag–Ag bonding, but it is significant enough to cause the ions to be triangular. We agree with Mason and Mingos,[19] who state "We do not and cannot distinguish, in general, the cases where a metal–metal bond order is due to direct overlap or to appropriate bridge bonding."

In Figure 3 we present a simplified MO diagram for Ag_2H^+ and show how it relates to the corresponding neutral molecules Ag_2 and AgH. All MOs of the cation are of course stabilized relative to those of the neutrals. In order to put the cation on a common scale, we have added a factor of 6.50 eV to the MOs of the cation so that the $4d_\delta$ orbitals of the cation are arbitrarily placed at the same energy as those of Ag_2.

An overlap population analysis on an orbital-by-orbital basis shows that each of these three molecules obtains the major share of bonding from a pair of σ-type orbitals. These are $3\sigma_g/4\sigma_g$ of Ag_2, $4a_1/7a_1$ of Ag_2H^+, and $3\sigma/4\sigma$ of AgH. For each pair of orbitals the first contains a large component of Ag 4d, whereas the second is predominantly Ag 5s. In Table I we present the major percentage of this pair of orbitals for Ag_2H^+ in terms of the fragment orbitals Ag_2 and H and the overlap population for each. (Similar data are given for $Ag_2CH_3^+$, which will be discussed shortly.) The bonding/antibonding among these major components can be seen easily from the sense of the correlation lines drawn in Figure 3. Pictorial representations of these two Ag_2H^+ orbitals are also shown in Figure 3.

The d^{10}–d^{10} portion of Ag_2 is strictly textbook-like.[20] The unusual features of Figure 3 relate to the stabilization of the 3σ MO in AgH (mainly $4d_\sigma$) from the corresponding mainly d_δ and

(19) Mason, R.; Mingos, D. M. P. *J. Organomet. Chem.* **1973**, *50*, 53.
(20) DeKock, R. L.; Gray, H. B. *Chemical Structure and Bonding*; Benjamin/Cummings: Menlo Park, CA, 1980; p 248.

Table I. Analysis of Important Bonding Orbitals in Ag_2H^+ and $Ag_2CH_3^+$ in Terms of Fragment Orbitals Ag_2/H^+ and Ag_2/CH_3^+

		Ag_2H^+			
MO	Overlap pop.	Percent Composition $3\sigma_g(\sim 4d)$	$4\sigma_g(\sim 5s)$	$2\pi_u(\sim 4d)$	$1s_H$
$4a_1$	0.158	26	0	33	37
$7a_1$	0.161	11	49	12	24
Total e^- occupation	—	1.86	0.97	1.87	1.22

		$Ag_2CH_3^+$				
		Percent Composition			CH_3	
MO	Overlap pop.[a]	$3\sigma_g(\sim 4d)$	$4\sigma_g(\sim 5s)$	$2\pi_u(\sim 4d)$	$1a_1$	$2a_1$
5a′	0.026	0	1	2	96	1
7a′	0.070	51	0	29	2	14
12a′	0.109	3	39	6	1	43
Total e^- occupation	—	1.97	0.82	1.86	2.00	1.27

[a] The overlap population is between the Ag atom and the CH_3 group.

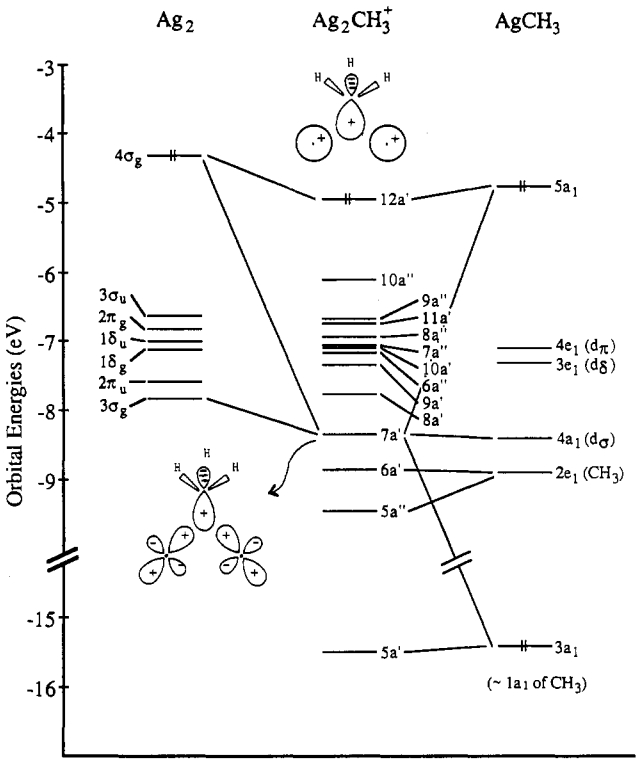

Figure 4. Molecular orbital correlation diagram for Ag_2, $Ag_2CH_3^+$, and $AgCH_3$.

d_π orbitals and even further stabilization of this MO ($4a_1$) in the case of Ag_2H^+. This, along with the orbital populations to be discussed shortly, is evidence of the importance of 4d orbital involvement in the bonding.

Figure 4 presents the corresponding MO diagram for Ag_2, $Ag_2CH_3^+$, and $AgCH_3$. Again, the major part of the bonding can be put to a pair of orbitals in the latter two species. In the $Ag_2CH_3^+$ ion these are 7a′ and 12a′; in $AgCH_3$ they are $4a_1$ and $5a_1$. (The MOs of $Ag_2CH_3^+$ have been shifted by 6.13 eV to scale the d_δ orbitals, as for Ag_2H^+.) The $AgCH_3$ MO diagram is practically a picture-perfect pattern of that for AgH. The main difference between $Ag_2CH_3^+$ and Ag_2H^+ is that the d^{10}–d^{10} set of MOs (7a′–10a″) are spread over 2.2 eV of energy, compared to only 1.3 eV for Ag_2H^+. This is an indication that the methyl group, with its more complicated set of frontier orbitals, is more capable of perturbing the 4d band than is the H atom. We further notice that the 7a′ orbital is not stabilized as much in a relative sense as was the $4a_1$ orbital of Ag_2H^+. This lack of stabilization

of 7a′ can be traced to a number of reasons. First, there is an antibonding interaction from the $1a_1$ fragment orbital of methyl. Second, there is a larger energetic difference between the methyl cation acceptor orbital ($2a_1$) and the $3\sigma_g$ donor orbital of Ag_2 than there is between the latter and the 1s orbital of H^+. A good indicator of this feature is that our calculated ionization energy for the H atom is 295.4 kcal/mol whereas that for the methyl cation is calculated to be 224.5 kcal/mol (see below). Third, the overlap integrals of the $2a_1$ methyl cation acceptor orbital with the $3\sigma_g$ and $2\pi_u$ donor orbitals of Ag_2 are 0.11 and 0.14, respectively. The corresponding values with the 1s orbital of H^+ are both 0.19. All three factors serve to destabilize the 7a′ orbital of $Ag_2CH_3^+$ relative to the corresponding $4a_1$ orbital of Ag_2H^+. This by itself does not mean that there is less bonding between the methyl fragment and the Ag_2 fragment than is the case for the H atom. In fact, part of this lost bonding is made up in a lower a′ orbital (5a′), which results from bonding between the $1a_1$ fragment orbital of the methyl group and the $3\sigma_g$ orbital of Ag_2. Table I contains the overlap population and percent composition of the pertinent MOs for $Ag_2CH_3^+$. These numbers, coupled with the MO diagram given in Figure 4, serve to provide a fairly complete picture of the bonding in $Ag_2CH_3^+$.

In Table I we present also the fragment orbital occupations for the same orbitals for which percent composition was given. Notice that the $3\sigma_g$ and $2\pi_u$ orbitals of Ag_2 have populations near 1.90. In the free diatomic these orbitals have 2.00 electrons; this drop in value along with the MO diagrams in Figures 3 and 4 indicates that the 4d orbitals are involved in the bonding in both Ag_2H^+ and $Ag_2CH_3^+$. The 5s orbital involvement is obviously large. Although we do not exhibit individual atomic orbital occupations for the Ag atoms, we observe that the 5p orbital occupation never exceeds 0.05 electron. It seems that there is little involvement of the 5p orbitals. This result is not too surprising in view of the similar lack of Au 6p orbital participation that we observed in the complex $Au(CH_3)(PH_3)$.[21]

Proton Affinity (PA) and Methyl Cation Affinity (MCA) of Ag_2. We have calculated the affinity of Ag_2 for H^+ and for CH_3^+ by doing the calculations in terms of the appropriate fragments. The HFS method has been used previously to compute proton affinities successfully.[22] Neither of the affinities reported here have been measured experimentally.

The PA of Ag_2 is calculated to be 193.5 kcal/mol, without zero-point energy correction. (Such a correction would lower the proton affinity by about 5 kcal/mol.) This places Ag_2 almost as basic as NH_3 (205 kcal/mol) for the gas-phase protonation reaction.[23]

Of further interest to us is the breakdown of the PA into an electronic and steric component. In order to carry out this analysis we need to "prepare" the substrate Ag_2 molecule before it is protonated. This amounts to lengthening of the Ag_2 bond from 2.70 to 2.86 Å and is endothermic by 2.6 kcal/mol. Hence, protonation of the "prepared" substrate amounts to 196.1 kcal/mol. This number can be broken down further into an electronic contribution from each symmetry block in the C_{2v} molecule and a total electrostatic interaction between the bare proton and the frozen electron density on the Ag_2 fragment. The breakdown is as follows:

		energy, kcal/mol
electronic	a_1	218.8
	a_2	1.0
	b_1	2.0
	b_2	6.1
steric		−31.9
total		196.1

The predominant orbital that H^+ uses for bonding is the 1s orbital, which belongs only to the a_1 representation, so it is not surprising that the a_1 representation is the most important. The steric term deserves comment. This term reflects the interaction of the bare proton with the frozen electron density of the Ag_2 substrate. At first glance it might be expected that this term should always be attractive, since the proton would be attracted to the electron cloud of the substrate. However, we calculate a repulsive steric term. Further reflection leads one to realize that this can happen in certain circumstances. Indeed, here we have the proton "buried" quite deeply in the valence electron cloud of the substrate so that the repulsion of the proton with the two Ag nuclei is greater than the attractive terms. It is unlikely that this effect would ever be observed for the attack of a proton at a *single* atom. In the work of Ziegler[22] this term was always attractive, but the proton attack was at a single atom. There are similar examples in which the electrostatic potential is destabilizing.[24] (The steric term in our analysis where one of the fragments is a proton is nothing other than what is referred to as the electrostatic potential elsewhere in the chemical literature.)

We turn next to a discussion of the MCA of Ag_2. A breakdown is given in the same way as for the proton affinity. The total interaction energy is 128.7 kcal/mol. Since 0.7 kcal/mol is required to lengthen the Ag_2 bond from 2.7 to 2.75 Å and 20.8 kcal/mol is required to pyramidalize the methyl cation, the MCA from the "prepared" fragments is 150.2 kcal/mol. The breakdown is as follows in the C_s point group:

		energy, kcal/mol
electronic	a′	211.0
	a″	13.7
steric		−74.5
total		150.2

The MCA is considerably less than the PA, in agreement with what is known about these two affinities.[25] The electronic portion of the MCA is actually greater than that of the PA. It is the steric term that is substantially more destabilizing for the methyl case. In addition, the methyl cation suffers from a "preparation energy"

Table II. Fragmentation Energies of the Parent Ions (kcal/mol)

$Ag_2H^+ \rightarrow Ag_2 + H^+$	193.5
$Ag_2H^+ \rightarrow Ag_2^+ + H$	58
$Ag_2H^+ \rightarrow AgH + Ag^+$	60
$Ag_2H^+ \rightarrow AgH^+ + Ag$	91
$Ag_2CH_3 \rightarrow Ag_2 + CH_3^+$	129
$Ag_2CH_3^+ \rightarrow Ag_2^+ + CH_3$	64
$Ag_2CH_3^+ \rightarrow AgCH_3 + Ag^+$	63
$Ag_2CH_3^+ \rightarrow AgCH_3^+ + Ag$	80

Table III. Relevant Dissociation Energies and Ionization Energies (kcal/mol)

	calcd[a]	exptl
$H \rightarrow H^+ + e^-$	295.4	313.5[b]
$CH_3 \rightarrow CH_3^+ + e^-$	224.5	226.0[c]
$Ag \rightarrow Ag^+ + e^-$	164.0	174.7[b]
$Ag_2 \rightarrow Ag_2^+ + e^-$	160.0	
$AgH \rightarrow AgH^+ + e^-$	195.0	
$AgCH_3 \rightarrow AgCH_3^+ + e^-$	180.5	
$Ag_2 \rightarrow 2Ag$	35.6	38[d]
$AgH \rightarrow Ag + H$	37.8	55.1[d]
$AgCH_3 \rightarrow Ag + CH_3$	40.9	

[a] The calculated ionization energies for molecules are vertical ionization energies. The dissociation energies are without zero-point energy corrections. [b] Moore, C. E. *Ionization Potentials and Ionization Limits Derived from the Analyses of Optical Spectra*; NSRDS-NBS 34; National Bureau of Standards: Washington, DC, 1970. [c] Houle, F. A.; Beauchamp, J. L. *J. Am. Chem. Soc.* **1979**, *101*, 4067. [d] Huber, H.; Herzberg, G. *Molecular Spectra and Molecular Structure*; Van Nostrand Reinhold: New York, 1979; Vol. IV.

(21) DeKock, R. L.; Baerends, E. J.; Boerrigter, P. M.; Hengelmolen, R. *J. Am. Chem. Soc.* **1984**, *106*, 3387.
(22) Ziegler, T. *Organometallics* **1985**, *4*, 675.
(23) Jenkins, H. D. B.; Morse, D. F. C. *J. Chem. Soc., Faraday Trans. 2* **1984**, *80*, 1167.
(24) Ramos, M. J.; Webster, B. *J. Chem. Soc., Faraday Trans. 2* **1983**, *79*, 1389. Politzer, P.; Kammeyer, C. W.; Bauer, J.; Hedges, W. L. *J. Phys. Chem.* **1981**, *85*, 4057.
(25) Berthod, H.; Pullman, A. *Isr. J. Chem.* **1980**, *19*, 299.

that is not present for the proton (20.8 kcal/mol).

Fragmentation of the Cations. In the Introduction we pointed out that Busch et al.[1] observed that CID of $Ag_2CH_3^+$ produced a significant fraction of Ag_2^+ daughter ions but that none were observed from Ag_2H^+. We have calculated the various fragmentation energies of the title cations, and these are shown in Table II. (For completeness' sake, we list the various dissociation energies and ionization energies that are relevant to this study in Table III.)[26] The resultant values show that there is not a distinct difference between the fragmentation energies of Ag_2H^+ and $Ag_2CH_3^+$. Also, recall from our earlier discussion that there is little difference between the ground-state structures of the two ions. Both Holmes[27] and Lorquet[28] have discussed the relationship between CID and structure specificity. The CID experiment involved a 20-eV collisions between argon atoms and the parent silver ion in the mass spectrometer chamber.[1] Most of the imparted translational energy will be converted into internal vibrational and rotational energy, which is then assumed to be rapidly randomized among the various vibrational modes of the molecule. The relative abundance of daughter ions is usually independent of the amount of internal energy imparted to the parent ion.

On purely statistical grounds, since the fragmentation energies of Ag_2H^+ to produce AgH^+ and Ag_2^+ are nearly identical, one might expect equal amounts of these daughter ions in the CID. The fact that no Ag_2^+ is observed indicates that one or more of the following is true: (1) Our calculated results are not trustworthy. (2) The fragmenting ion with varying degrees of vibrational and rotational excitation does not retain the structure of the ground state. This could occur if the barrier for interconversion between two isomers (e.g., in our case triangular Ag_2H^+ and linear $AgHAg^+$) is considerably lower than that for decomposition. As discussed above, this interconversion barrier is indeed much lower for Ag_2H^+ than for $Ag_2CH_3^+$. (3) There is a kinematic effect whereby the relatively large argon atom is presented with a small collisional cross section by the H atom in Ag_2H^+. Consequently, the vibrational energy might not be randomized among the various vibrational modes of the fragmenting ion. Preferential Ag–Ag bond breaking could occur rather than that of Ag–H.

Acknowledgment. This work was supported in part by the Natural Sciences and Engineering Research Council of Canada (NSERC), who provided an International Exchange Award to R.D.K. Acknowledgment also is made to the donors of the Petroleum Research Fund, administered by the American Chemical Society, for partial support of this research. Thanks are also due to SuperComputing Services of the University of Calgary for the allocation of computer time on the Cyber 205. R.D.K. wishes to thank Calvin College for released time to work on this project.

(26) It is evident from Table III that some of the calculated values are in error by 10–18 kcal/mol compared to experiment. Since several values in Table III have no experimental counterpart, it is difficult to know whether or not we are introducing a systematic error into the fragmentation energies presented in Table II. In each of the five cases where a comparison can be made with experiment, we underestimate the experimental quantity. Since we are really only interested in *relative* fragmentation energies, it may well be that these errors are tending to cancel each other.

(27) Holmes, J. L. *Org. Mass Spectrom.* **1985**, *20*, 169.

(28) Lorquet, J. C. *Org. Mass Spectrom.* **1981**, *16*, 469. Lorquet, J. C. *Mass Spectrometry*; Royal Society of Chemistry: London, 1984; Vol. 7, p 63.

Contribution from the Institut für Physikalische und Theoretische Chemie, Technische Universität Braunschweig, D-3300 Braunschweig, Federal Republic of Germany

Assignment of the Valence Ionization Spectrum of $TiCl_4$

W. von Niessen

Received July 3, 1986

The ionization energies and relative intensities in the valence region of $TiCl_4$ are calculated by an ab initio many-body Green's function formalism that takes the effects of electron correlation and relaxation into account. The calculations are based on a SCF wave function obtained with a double-ζ basis set. The ordering of the ionic states in the outer valence region is $1t_1 < 3t_2 < 1e \approx 2t_2 < 2a_1$. In the inner valence region, i.e. for the orbitals $1t_2$ and $1a_1$, we observe the typical breakdown of the molecular orbital model of ionization. The intensity becomes distributed over many states.

Introduction

Among the molecules involving a transition-metal atom, the $TiCl_4$ molecule is a very simple and fundamental one. The understanding of the electronic structure of this molecule is thus of considerable importance. In spite of a fairly large number of investigations, however, several aspects of the electronic structure could not be clarified unambiguously. Among these is the assignment of the valence photoelectron spectrum (PES). This is due to the large number of states crowded in a narrow energy interval. The He I and also the He II photoelectron spectra of $TiCl_4$ have been reported and discussed repeatedly.[1-6] However, some points in the interpretation of the spectrum are still not settled[6] (see also ref 7). A large number of calculations of semiempirical, discrete variational $X\alpha$ (DVM–$X\alpha$), SCF–$X\alpha$, and ab initio type have been performed,[4,6,8-17] but the sequence of orbital energies disagreed among the different calculations. Essentially two different assignments are at present proposed for the valence bands named A, B, (C + D), and E by Egdell et al.[1] As the bands C and D are very closely spaced and overlap, the ordering of the states assigned to these bands has generally not been specified. The first assignment is $1t_1$ (A), $3t_2$ (B), ($1e + 2t_2$) ((C + D)), and $2a_1$ (E). This ordering of states is supported by the experimental results of ref 1–5 and the investigation using synchrotron radiation by Lübcke et al.,[40] who derived this result from the energy dependence of the partial photoionization cross sections, and it is obtained by the calculations with DVM–$X\alpha$,[13,14]

(1) Egdell, R. G.; Orchard, A. F.; Lloyd, D. R.; Richardson, N. V. *J. Electron Spectrosc.* **1977**, *12*, 415.
(2) Cox, P. A.; Evans, S.; Hamnett, A.; Orchard, A. F. *Chem. Phys. Lett.* **1970**, *7*, 414.
(3) Green, J. C.; Green, M. L. H.; Joachim, P. J.; Orchard, A. F.; Turner, D. W. *Philos. Trans. R. Soc. London, A* **1970**, *No. 268*, 111.
(4) Burroughs, P.; Evans, S.; Hamnett, A.; Orchard, A. F.; Richardson, N. V. *J. Chem. Soc., Faraday Trans. 2* **1974**, *70*, 1895.
(5) Egdell, R. G.; Orchard, A. F. *J. Chem. Soc., Faraday Trans. 2* **1978**, *74*, 485.
(6) Bancroft, G. M.; Pellach, E.; Tse, J. S. *Inorg. Chem.* **1982**, *21*, 2950.
(7) Cowley, A. H. *Inorg. Chem.* **1979**, *26*, 45.
(8) Becker, C. A. L.; Dahl, J. P. *Theor. Chim. Acta* **1969**, *14*, 26.
(9) Becker, C. A. L.; Ballhausen, C. J.; Trabjerg, I. *Theor. Chim. Acta* **1969**, *13*, 355.
(10) Choplin, F.; Kaufmann, G. *Theor. Chim. Acta* **1972**, *25*, 54.
(11) Truax, D. R.; Geer, J. A.; Ziegler, T. *J. Chem. Phys.* **1973**, *59*, 6662.
(12) Fenske, F. R.; Radtke, D. D. *Inorg. Chem.* **1968**, *7*, 479.
(13) Ellis, D. E.; Parameswan, T. *Int. J. Quantum Chem., Symp.* **1971**, *5*, 443.
(14) Parameswan, T.; Ellis, D. E. *J. Chem. Phys.* **1973**, *58*, 2088.
(15) Tossell, J. A. *Chem. Phys. Lett.* **1979**, *65*, 371.
(16) Foti, A. E.; Smith, V. H.; Whitehead, M. A. *Mol. Phys.* **1982**, *45*, 385.
(17) Hillier, I. H.; Kendrick, J. *Inorg. Chem.* **1976**, *15*, 520.

0020-1669/87/1326-0567$01.50/0